IET Nanobiotechnology

Research Article

IET Journals
The Institution of Engineering and Technology

Surface stress-induced membrane biosensor based on double-layer stable gold nanostructures for *E. coli* detection

ISSN 1751-8741
Received on 2nd March 2019
Revised 22nd July 2019
Accepted on 26th July 2019
E-First on 11th October 2019
doi: 10.1049/iet-nbt.2019.0096
www.ietdl.org

Dong Zhao[1], Yan Liu[1], Zhen Pei[1], Qiang Zhang[1], Yixia Zhang[1], Wendong Zhang[1], Shengbo Sang[1,2] ✉

[1]MicroNano System Research Center, Key Lab of Advanced Transducers and Intelligent Control System of the Ministry of Education & College of Information and Computer, Taiyuan University of Technology, Taiyuan, People's Republic of China

[2]Department of Pathology, Brigham and Women's Hospital/ Harvard Medical School, Boston, MA, USA

✉ *E-mail: sunboa-sang@tyut.edu.cn*

Abstract: The surface stress-based biosensor has been applied in fast and sensitive identification of *Escherichia coli* (*E. coli*)with significance for public health, food, and water safety. However, the stable sensitive element of flexible biosensor based on surface stress is still crucial and challengeable. Here, the authors reported surface stress-induced biosensors based on double-layer stable gold nanostructures (D-AuNS-SSMB) for *E. coli* O157:H7 detection. Bacterial detection demonstrates the high stability of the biosensor. The resistance change of biosensor is linear to the logarithmic value of the *E. coli* O157:H7 concentrations ranging from 10^3 to 10^7 CFU/mL with a limit of detection (LOD) of 43 CFU/mL. The captured signals of D-AuNS-SSMB comes from surface stress generated by antigen–antibody binding. In addition, the biosensor exhibits good stability, reproducibility and specificity in detection of *E. coli* O157:H7 as well. This study provides a new preparation method of stable sensitive element for the *E. coli* detection.

1 Introduction

Surface stress-induced biosensors hold remarkable potential for diverse applications in biomolecules and cell detection due to their label-free technology, direct detection method, and simple preparation [1–7]. The biosensor depends on the deformation of the sensitive element to sense surface stress generated during the biomolecule interactions [8–11]. Hence, the stability and consistency of the sensitive element surface play a significant role in improving the performance of the surface stress-induced biosensors [12, 13].

Currently, numerous researches have been conducted to improve the surface stability of the sensitive element. Tsouti *et al.* [14] deposited a passivation layer of silicon dioxide to coat sensitive element and effectively improved the stability of the surface stress-induced biosensors. However, the silicon dioxide, as a protective layer, increased the thickness of the sensitive element, leading to the decrease in the biosensor sensitivity. Loizeau *et al.* selected silicon membrane to sense surface stress and employed functionalisation polymer to protect the stability of sensitive element [15]. Due to the swelling of functionalisation polymer, the signal-to-noise ratio of the surface stress-induced biosensors was reduced, and the experimental errors increased. Other works deposited gold nanoparticles on polydimethylsiloxane (PDMS) to fabricate sensitive element of surface stress-induced biosensors, due to simple preparation, non-toxic and biocompatibility [16–19]. However, instability and abscission of the gold nanoparticles on PDMS are prone to break the interface balance of sensitive element, and restrain sensitivity of surface stress-induced biosensors and increase the signal-to-noise ratio of the sensing system.

Herein, we prepared double-layer stable gold nanostructures (D-AuNS) on PDMS surface via two-step reduction method and constructed surface-stable biosensors. The biosensor was employed to specifically detect *Escherichia coli* O157:H7 *(E. coli* O157:H7*)* based on the surface stress. The performance of the stable sensitive elements was demonstrated by measuring the response of the biosensor to the bacterium. The biosensor was characterised by ultraviolet–visible (UV-Vis) spectrophotometry and scanning electron microscope (SEM) in detail. Furthermore, the mechanism of surface stress sensing was discussed. The surface stress-induced biosensor based on double-layer stable gold nanostructures (D-AuNS-SSMBs) is sensitive to *E. coli* O157:H7, which demonstrates the potential for practical applications in monitoring the *E. coli* O157:H7 concentration.

2 Material and methods

2.1 Materials

PDMS (Sylgard 184 silicone elastomer kit) was obtained from Dow Corning (Midland, MI, USA). Chloroauric acid tetrahydrate ($HAuCl_4{\cdot}4H_2O$, Au≥47.8%) was purchased from Sinopharm Chemical Reagent Co., Ltd (Shanghai, CHN). D-Glucose ($C_6H_{12}O_6{\cdot}H_2O$, ≥99.5%) was purchased from Hengxing Chemical Reagents (Tianjin, CHN). Potassium bicarbonate ($KHCO_3$, ≥99.5%) was purchased from Fuchen Chemical Regents (Tianjin, CHN). 11 Mercapto 1 undecanoicacid (MUA: SH-$(CH_2)_{10}$-COOH) was provided by Nanjing pars Biotechnology Co., Ltd 1-ethyl-3-carbodiimide (EDC), N-hydroxysulfosuccinimide (NHS), and *E. coli* antibody (anti-*E. coli*) were obtained from Hushi (Shanghai, China). Bovine serum albumin (BSA) was provided by Sigma-Aldrich (Saint Louis, MO, USA). *Clostridium botulinum* (*C. botulinum*), *Salmonella enteritidis* (*S. enteritidis*), and *Staphylococcus aureus* (*S. aureus*) were provided by Institute of Microbiology, Chinese Academy of Sciences. Deionised water was purified using the Ulupure ultrapure water system (resistivity, 18.25 MΩ·cm). All other chemicals and solvents were reagent grade or of higher quality and used as received.

2.2 Fabrication of D-AuNS-SSMBs

The mixture solution of Sylgard 184 monomer and curing agent in a weight ratio of 10:1 was prepared and removed the air bubbles in vacuum at room temperature. PDMS films were fabricated by spinning mixed solution on glass substrates at 2000 rpm for 1.5 min by spin coater (SPIN-1200D, Midas, Daejeon, Korea) and then cured at 70°C for 3 h. The Au-seeds, as the first layer of AuNS, were generated in PDMS films by immersing the cured native PDMS films in 0.01 g/mL $HAuCl_4$ alcohol solution for 24 h at room temperature. The Au-seed PDMS films were transferred from the glass substrate to the cured pure PDMS, which had circular

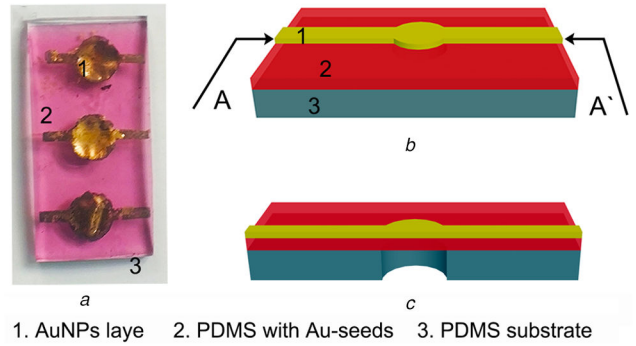

Fig. 1 *Schematic representation of the D-AuNS-SSMB*
(a) Photographic image of the D-AuNS-SSMB, ***(b)*** Schematic diagram and cutaway drawing of the D-AuNS-SSMB, ***(c)*** The cross-section view of AA

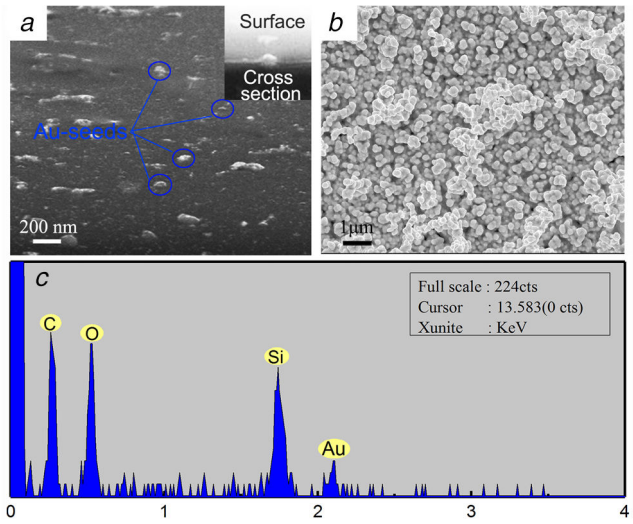

Fig. 2 *SEM characterisation of D-AuNS-SSMB*
(a) SEM image of the first layer of AuNSs. The inset shows the cross section of PDMS with the first layer of AuNSs, ***(b)*** SEM image of the second layer of AuNSs on the D-AuNS-SSMB surface by glucose reduction, ***(c)*** EDS of the D-AuNS-SSMB with the first layer of AuNSs

holes in order to facilitate the deformation of the film. The second layer of AuNS on PDMS continued to grow on the basis of Au-seeds in the mixed solution, containing glucose (0.02 g/mL), $KHCO_3$ (0.02 g/mL) and $HAuCl_4$ (0.01 g/mL). The pH of the solution was adjusted to 9.0 by dripping 0.01 g/ml NaOH solution and kept for 20 min at 0–4°C. The photographic image and schematic of D-AuNS-SSMB are shown in Fig. 1.

2.3 Characterisation of the PDMS films with gold nanostructures (AuNS-PDMS)

The surface morphology of AuNS-PDMS films were characterised by SEM (JSM-7400F, JEOL, Japan) at 10 kV. The absorption peak of D-AuNSs of the composite films, which is located in 540 nm wavelength, were tested utilising UV-Vis spectroscopy (UV-3100, Shimadzu, Japan) at room temperature. Digital Multimeter (Keithley 2400, Tektronix, USA) was purchased to test the electrical characteristics.

2.4 Functionalisation of D-AuNS-SSMB

The D-AuNS-SSMBs were cleaned for 5 min by successively soaking in acetone, isopropanol, alcohol, and deionised water and dried with nitrogen, followed by incubating in 0.1 mM MUA for 10 h to form the self-assembled monolayer. MUA-modified D-AuNS-SSMBs were activated by incubating in a mixture solution of 3 mg/mL EDC and 3 mg/mL NHS (volume ratio = 1:1) for 1 h at room temperature, and then injected 1 mg/mL anti-*E.coli* and kept for 1 h at 37°C. Afterwards, the biosensors were incubated in 0.1% BSA for 1 h. The biosensors were rinsed with ethanol and deionised water to remove the free MUA and anti-*E.coli*, and dried with nitrogen finally.

2.5 Bacterial culture

E. coli O157:H7 was cultured in Luria-Bertani media at 37°C overnight in cell culture incubator (HERAcell150i, Thermo, USA), and centrifuged at 5000 rpm for 2 h, followed by resuspension in 25 mL normal saline. The bacterial suspensions with different concentrations were diluted with normal saline as well.

2.6 E. coli O157:H7 detection

The D-AuNS-SSMBs were exposed to the *E. coli* O157:H7 with concentration ranging from 10^3 to 10^7 CFU/mL for 30 min. Then the Digital Multimeter (2400, Keithley Instrument, Ohio, USA) was employed to detect the response of D-AuNS-SSMB to *E. coli* O157:H7 with concentrations ranging from 10^3 to 10^7 CFU/mL. The *I–V* curves were obtained by voltage scanning measurement. The resistances (R) were calculated according to the measured *I–V* curves. The resistance change ($\Delta R/R_0$) of D-AuNS-SSMB is obtained with $(R–R_0)/R_0$ calculation, where R the resistance of biosensors with different bacterial concentrations, and R_0 is the initial resistance of biosensor. The standard deviation is calculated with (1).

$$\sigma = \sqrt{\frac{1}{n}\sum_{i=1}^{n}(\Delta R_i/R_0 - \overline{\Delta R/R_0})} \tag{1}$$

Where σ is the standard deviation, n is the number of parallel experimental tests and $n = 10$ in this study, $\Delta R_i/R_0$ is the resistance change and $\overline{\Delta R/R_0}$ is the average resistance change of the biosensor in ten parallel experiments at the same bacterial concentration.

3 Results and discussion

3.1 Growth of D-AuNSs

As well-known, the Si-H groups are enriched in cured PDMS and considered as the reducing agent [20]. Herein, PDMS can in situ reduce $HAuCl_4$ to gold nanoparticles (2) [21], which forms the first layer of AuNS (Fig. 2*a*). The gold nanoparticles in the first layer of AuNS are regarded as the Au-seeds and embedded into the PDMS surface (inset in Fig. 2*a*). Furthermore, the energy dispersive spectrometer (EDS) in Fig. 2*c* shows that the composite films include gold atoms, proving that AuNSs are reduced in PDMS. Based on the Au-seeds, the D-AuNSs are continually constructed to form the second layer of AuNS by glucose reduction (Fig. 2*b*). The reduction process is described as (3). The D-AuNSs grows steadily on the PDMS surface due to the embedded Au-seeds. Absorption of carbon dioxide by NaOH solution and reduction of reaction rate at low temperature contribute to uniformly distribute of D-AuNSs on the PDMS surface.

$$\begin{aligned} &4AuCl_4^- + 6 - \overset{|}{\underset{|}{Si}} - H + 3H_2O \rightarrow 4Au \\ &+3 - \overset{|}{\underset{|}{Si}} - O - \overset{|}{\underset{|}{Si}} - + 16Cl^- + 12H^+ \end{aligned} \tag{2}$$

$$\begin{aligned} &2HAuCl_4 + 3HOCH_2(CHOH)_4CHO \rightarrow 2Au \\ &+3HOCH_2(CHOH)_4COOH + 8HCl + H_2O \end{aligned} \tag{3}$$

To further characterise D-AuNSs, the AuNS-PDMS films were tested with typical UV-Vis spectroscopy, as shown in Fig. 3. It can be seen in Fig. 3 that the AuNS-PDMS with the first layer of AuNSs has an absorption peak at 540 nm due to the surface plasmon resonance of gold nanoparticles in PDMS films [22], compared with PDMS film without AuNSs. The absorption peak of AuNSs is enhanced with glucose reduction, indicating the formation of the second layer of AuNSs.

The gold stability of AuNSs-PDMS film prepared by two-step reduction is compared with that prepared by one-step reduction of

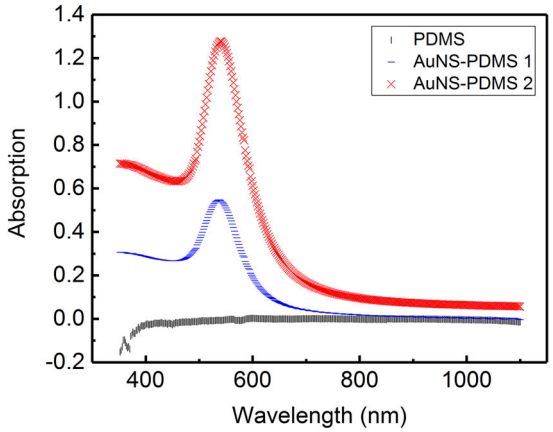

Fig. 3 *UV-Vis spectroscopy of PDMS, PDMS with the first layer of AuNSs and PDMS with the second layer of AuNSs*

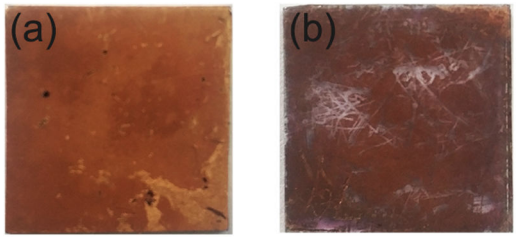

Fig. 4 *Photographic image of AuNS-PDMS film*
(a) AuNS-PDMS prepared by two-step reduction method, ***(b)*** AuNS-PDMS prepared by one-step reduction of glucose

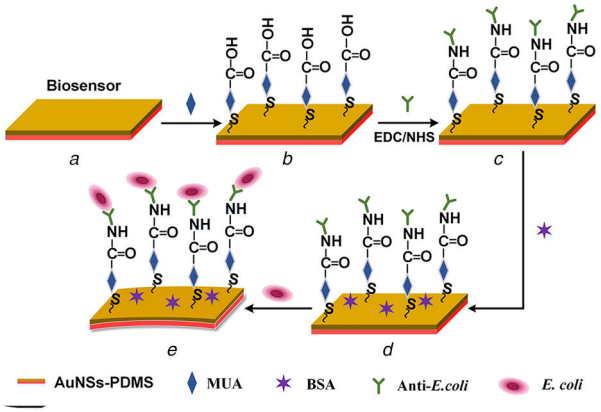

Fig. 5 *Schematic diagram of the modification procedure of the D-AuNS-SSMB*

glucose, as shown in Fig. 4. The film demonstrates a stable gold layer on the PDMS surface due to D-AuNS; however, the film suffers from a gold layer falling off the PDMS surface due to weak adsorption between monolayer AuNS and PDMS. At present, many similar sensors stabilise the gold layer by evaporation of chromium plating; however, evaporation process has a negative impact on the sensitivity of the biosensor due to the increase of film thickness [23, 24]. Therefore, two-step reduction can effectively improve the stability of AuNSs on PDMS surface.

3.2 Response principle of the biosensing strategy

The process of functionalisation and specific binding with *E. coli* O157:H7 are shown in Fig. 5. Initially, hydroxyl (-COOH) groups are immobilised on the D-AuNS-SSMB surface via self-assembling of MUA [25, 26], as shown in Figs. 5*a* and *b*. Then anti-*E.coli* is assembled on the carboxylated D-AuNS-SSMB by chemical treatment of EDC/NHS solution, forming a specific recognition interface, as shown in Fig. 5*c*. The BSA is employed to inhibit non-specific binding and enhances the performance of specific recognition (Fig. 5*d*). *E. coli* can be specifically recognised and captured on the D-AuNS-SSMB surface.

Although great effort has been invested to apply to surface stress in biosensing, the generation mechanisms of surface stress, surface deformation process and force-electricity conversion method remain unclear. Our D-AuNS-SSMB provides a means to understand the generation mechanisms of surface stress [20, 26]. In the process of specific binding of *E. coli* O157:H7 with anti-*E.coli*, large bond energy emerges on D-AuNS-SSMB surface due to antigen–antibody binding, and is stronger than that between surface D-AuNSs, leading to the mutual exclusion of D-AuNSs on the surface [20]. As a result, compressive surface stress is generated on the D-AuNS-SSMB surface, causing a convex deformation of the membrane [26], as shown in Fig. 5*e*. The deformation of the membrane can inevitably hold change in the distance between the AuNSs on D-AuNS-SSMB surface, which turns into resistance changes finally. Therefore, the principle of D-AuNS-SSMB resistance change can be used to detect *E. coli* with different concentrations.

3.3 E.coli O157:H7 detection using D-AuNS-SSMBs

Before the *E.coli* detection, we first proved that the detection signals came from specific capture of *E.coli* O157:H7 via anti-*E.coli*. Hence, control experiments were designed and conducted. The *E.coli* O157:H7 (10^7 CFU/mL) was injected on anti-*E.coli*-modified D-AuNS-SSMB and anti-*E.coli*-free D-AuNS-SSMB, respectively, and the dynamic responses of the D-AuNS-SSMB are shown in Fig. 6*a*. The baseline was obtained by detecting normal saline with as-prepared D-AuNS-SSMB modified with anti-*E.coli*. The baseline reveals that gravity of normal saline contributes to 0.01 resistance change of the D-AuNS-SSMB. Due to the specific binding of *E.coli* O157:H7 and anti-*E.coli*-modified D-AuNS-SSMB, upward surface stress is generated and gradually increases to counteract gravity of bacterial solution. At 20 min, the upward surface stress is equal to gravity, and the film hardly deforms. Hence, the resistance of D-AuNS-SSMB restores the initial value. The upward surface stress continues to increase and exceeds the gravity, leading to convex deformation and re-rising resistance of the D-AuNS-SSMB. After 30 min, upward surface stress stabilises and resistance remains unchanged [24]. Therefore, the surface stress is considered as the ultimate cause of D-AuNS-SSMB resistance change. However, due to the absence of antigen–antibody specific binding and the generation of surface stress, the dynamic response of the anti-*E.coli*-free D-AuNS-SSMB to bacteria is the same as that of the normal saline. After the *E.coli* O157:H7 was incubated for 30 min, we removed the buffer and rinsed it with deionised water, and re-measured the change in resistance of the D-AuNS-SSMB, as shown in Fig. 6*b*. The resistance change of anti-*E.coli*-modified D-AuNS-SSMB is distinguished from the anti-*E.coli*-free D-AuNS-SSMB with the high signal difference, which further reveals that resistance change results from the specific capture of *E.coli* O157:H7.

The responses of *E. coli* O157:H7 with concentration ranging from 10^3 to 10^7 CFU/mL to D-AuNS-SSMB were monitored by resistance change. The *E. coli* O157:H7 was incubated on the D-AuNS-SSMB for 30 min and then washed to remove the buffer. Under the same conditions, each *E. coli* O157:H7 concentration was detected five times or more using as-prepared D-AuNS-SSMB. The response curve corresponding to resistance change of D-AuNS-SSMB within ten minutes versus the *E. coli* O157:H7 concentrations ranging from 10^3 to 10^7 CFU/mL is shown in Fig. 7. The resistance change of D-AuNS-SSMB is linear to the logarithmic value of the *E. coli* O157:H7 concentrations ranging from 10^3 to 10^7 CFU/mL. The linear equation can be represented by $\Delta R/R = 0.0057 \log C_{\text{E.coli}} + 0.0054$, with an R^2 value of 0.9849. Due to the specific binding between *E.coli* and anti-*E.coli*, the surface stress generates and plays a vital role in resistance increase of D-AuNS-SSMBs. Moreover, the experimental error in the process of *E. coli* O157:H7 detection is within the controllable range, which indicates that our D-AuNS-SSMB exhibits good repeatability. In addition, a statistical analysis was operated by the

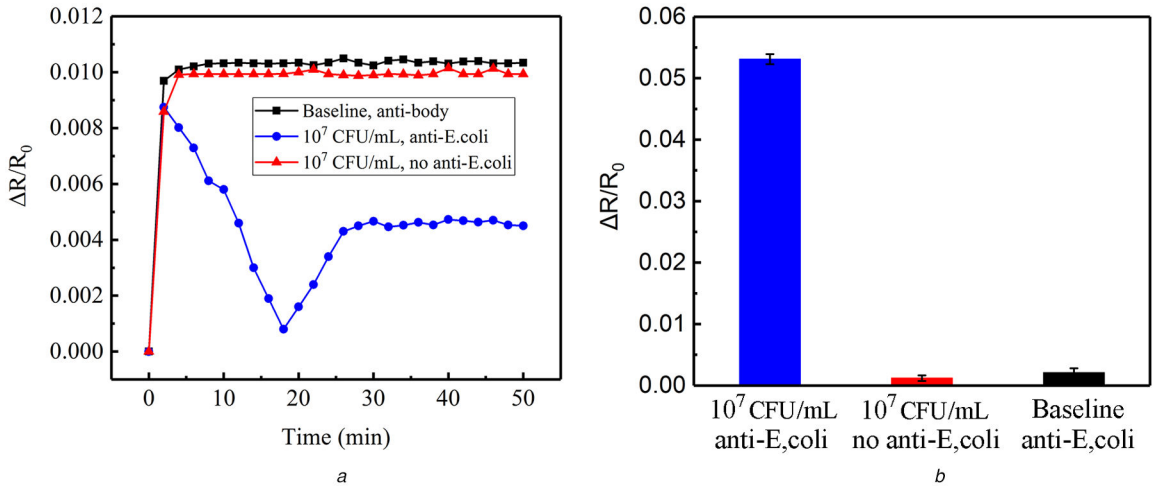

Fig. 6 *Response of the anti-E.coli-modified and anti-E.coli-free D-AuNS-SSMBs to E. coli O157:H7*
(a) The dynamic response *process,* ***(b)*** The resistance change of anti-*E. coli*-modified and anti-*E.coli*-free D-AuNS-SSMBs under the absence of buffer

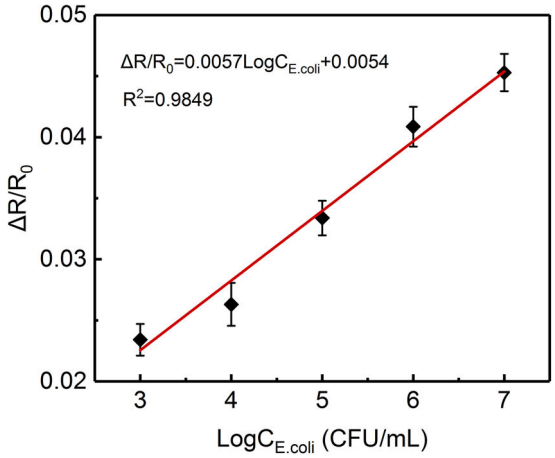

Fig. 7 *Response curve corresponding to resistance change of D-AuNS-SSMB within ten minutes versus the E. coli O157:H7 concentrations ranging from 10^3 to 10^7 CFU/mL*

Table 1 Comparison of the different methods for bacterium detection

Methods	LOD	Detection range	Time	References
PDMS surface stress biosensor	10^3 CFU/μL	10^3–8×10^3 CFU/μL	30 min	[24]
microcantilever biosensor based on surface stress	10^6 CFU/mL	10^6–2×10^8 CFU/mL	2 h	[28]
PEG-SH-coated cantilever	10^6 CFU/mL	10^6–10^8 CFU/mL	16 min	[29]
surface plasmon resonance (SPR)	10^4 CFU/mL	10^4–10^8 CFU/mL	<1 min	[30]
field-effect transistor device	10^3 CFU/mL	10^3–10^5 CFU/mL	NR	[31]
label-free SERS detection	10^5 CFU/mL	10^5–10^7 CFU/mL	3 h incubation	[32]
d-AuNS-SSMB	43 CFU/mL	10^3–10^7 CFU/mL	30 min	this work

NR, not recorded.

t-test method for five concentrations at a 95% confidence interval. The calculation results show $p<0.05$, which reveals that the resistance change has a statistical difference for different *E.coli* concentrations. The limit of detection (LOD) of D-AuNS-SSMB reaches 43 CFU/mL with $10^{3\sigma/S}$ calculation, where σ is the response standard deviation of $\log C_{\text{E.coli}}$ of the baseline, and S is the slope of the linear curve [27]. Moreover, the biosensor has shown excellent stability (Fig. S1). These results prove that D-AuNS-SSMB is a reliable method for high-performance *E.coli* detection.

We compared the performance of the D-AuNS-SSMB with the latest reports on the detection of the bacterium [24, 28, 29] (Table 1). PDMS surface stress biosensor was prepared stable and non-exfoliating gold electrodes on the chromium layer; however, the chromium layer increased the thickness of the film, leading to the poor bacterial sensitivity and the LOD [24]. Our D-AuNS-SSMB enjoys stable gold layer through the double-layer structure to avoid the shortcoming of thickness change and exhibits LOD of two orders of magnitude lower. Compared with D-AuNS-SSMB surface stress biosensors based on micro cantilever suffer from a narrower range of bacterial detection due to unstable gold layer [28, 29]. The LOD of D-AuNS-SSMB demonstrates a great advantage over cantilever surface stress biosensors as well. In addition, the performance of the D-AuNS-SSMB was compared with the existing methods [30–32], as shown in Table 1. Surface plasmon resonance and field-effect transistor device for *E. coli* detection exhibit poor detection range, LOD and sensitivity except requiring expensive and non-portable instrument [30, 31]. Label-free SERS method shows the same problems as well and requires the incubation time of over 3 h [32]. In comparison, the newly developed D-AuNS-SSMB in this work was prepared simply and

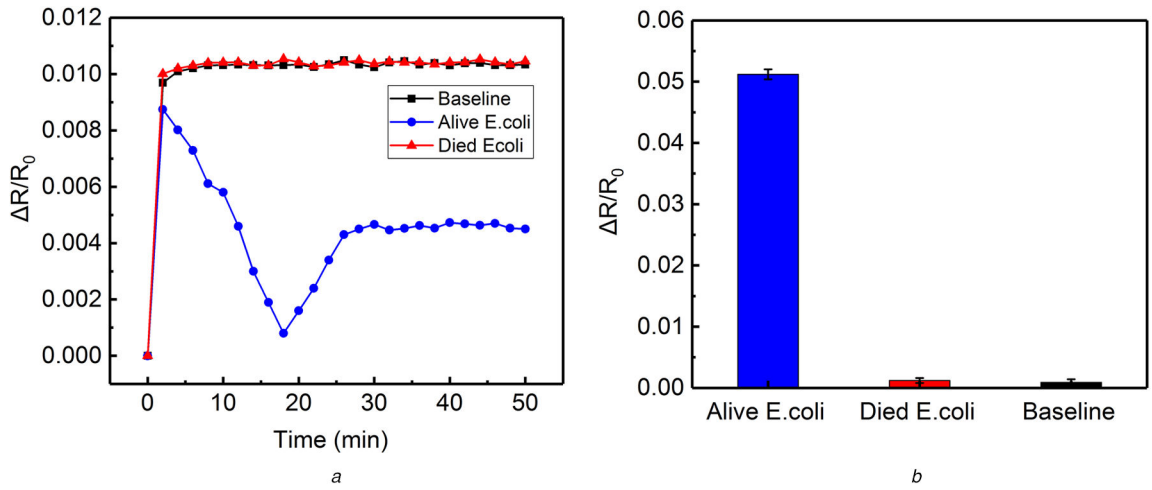

Fig. 8 *Dynamic responses of D-AuNS-SSMB to alive and died E. coli O157:H7*
(a) Dynamic response process, ***(b)*** The effects of *alive and dead E. coli* O157:H7 on D-AuNS-SSMB resistance change under the absence of buffer

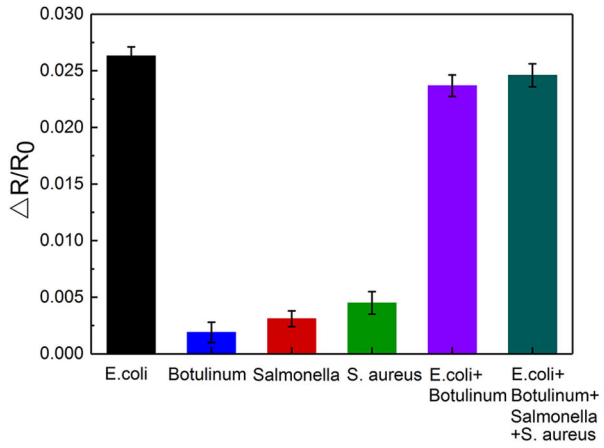

Fig. 9 *Resistance changes of D-AuNS-SSMB caused by different bacterial species*

has a convenient detection process. The sensor has shown a reliable sensitivity, and importantly, the performance achieved a LOD as low as 43 CFU/mL.

3.4 Study on the effect of E. coli O157:H7 activity on D-AuNS-SSMB

The activity of the *E. coli* has a significant effect on the D-AuNS-SSMB sensitivity due to inactivation of a specific protein of *E. coli* after high temperature sterilisation. Here, dead *E. coli* O157:H7 (10^7 CFU/mL) was obtained by heat inactivating the bacterial suspension with a different concentration in boiling water for 40 min. Comparing the alive *E. coli* O157:H7, the dynamic response of D-AuNS-SSMB to died *E. coli* O157:H7 is similar to that of normal saline (baseline), and the resistance of biosensor remains the same due to no generation of surface stress, as shown in Fig. 8*a*. Hence, the D-AuNS-SSMB exhibits non-specificity to dead *E. coli* O157:H7. After the alive and died *E.coli* O157:H7 were kept for 30 min, the buffer was washed out with saline and resistance changes of D-AuNS-SSMBs were measured and compared (Fig. 8*b*). It is clear that active *E. coli* causes more significant resistance changes than dead *E. coli* O157:H7 (Fig. 8*b*), indicating the insensitivity of D-AuNS-SSMB to dead *E. coli* O157:H7.

3.5 Specificity and selectivity of the D-AuNS-SSMB

The specificity of D-AuNS-SSMB was demonstrated by monitoring the responses of D-AuNS-SSMB to *E. coli* O157:H7, *C. botulinum*, *S. enteritidis*, and *S. aureus*, each at a concentration of 10^4 CFU/mL. Four bacteria were incubated on the D-AuNS-SSMB for 30 min and then washed to remove the buffer. The resistance changes of D-AuNS-SSMB are shown in Fig. 9. The D-AuNS-SSMB has a resistance change of 0.026 caused by *E. coli* O157:H7 and exhibits a sensitive response to the *E. coli* O157:H7; however, they have an indistinctive response to other bacteria due to their only non-specific adsorption. Hence, D-AuNS-SSMBs have a satisfactory specificity to *E. coli* O157:H7. In addition, the selectivity of D-AuNS-SSMB was demonstrated with pre-mixed suspensions of *E. coli* O157:H7, *C. botulinum*, *S. enteritidis,* and *S. aureus*. The D-AuNS-SSMB exhibits a resistance change of 0.023 and 0.024 against pre-mixed suspensions of all bacterium, which is almost identical to that against only *E. coli*, indicating a high-performance selectivity of the biosensor. In addition, when the concentration ratio of *E.coli* O157:H7 to *C. botulinum* varies between 10:1 and 10^4:1, the *C. botulinum* can not interfere with *E.coli* O157:H7 detections (Fig. S2). Therefore, the D-AuNS-SSMB can effectively detect *E. coli* O157:H7 in complex samples.

4 Conclusion

In this study, a D-AuNS-SSMB was fabricated for sensitive detection of *E. coli* O157:H7, with a stable sensitive element. The captured signals of D-AuNS-SSMB were proven to come from surface stress generated by antigen–antibody binding, further demonstrating the stability of the biosensor. The D-AuNS-SSMB demonstrates a linear response to the logarithmic value of the *E. coli* O157:H7 concentrations ranging from 10^3 to 10^7 CFU/mL with a LOD of 43 CFU/mL, and exhibits high-performance repeatability and specificity. The study not only provides a new detection method for *E coli*, but also indicates its potential application in water quality monitoring. In addition, the application of the D-AuNS-SSMBs in complex samples or real water samples will be further studied as our future work.

5 Acknowledgments

The authors are grateful for the support by the National Natural Science Foundation of China (nos. 51622507, 61471255, 61703298, 61474079), the Basic Research Program of Shanxi for Youths (no. 201701D221110); the Excellent Talents Technology Innovation Program of Shanxi Province of China (no. 201605D211023), and 863 project (no. 2015AA042601).

6 References

[1] Khansili, N., Rattu, G., Krishna, P.M.: 'Label-free optical biosensors for food and biological sensor applications', *Sens. Actuators. B-Chem*, 2018, **265**, pp. 35–49

[2] Li, C., Chen, X., Zhang, Z., *et al.*: 'Gold nanoparticle-DNA conjugates enhanced determination of dopamine by aptamer-based microcantilever array sensor', *Sensor Actuat. B-Chem*, 2018, **275**, pp. 25–30

[3] Said, F.A., Menon, P.S., Rajendran, V., *et al.*: 'Investigation of graphene-on-metal substrates for spr-based sensor using finite-difference time domain', *IET Nanobiotechnol.*, 2017, **11**, (8), pp. 981–986

[4] Bisen, M., Ansari, M.Z.: 'Phenomenological modelling sensitivity of su8/Cb nanocomposite conducting polymer microcantilever biosensor', *Mater.Today: P.*, 2017, **4**, (9), pp. 10395–10399
[5] Mertens, J., Rogero, C., Calleja, M., *et al.*: 'Label-free detection of DNA hybridisation based on hydration-induced tension in nucleic acid films', *Nat. Nanotechnol.*, 2008, **3**, p. 301
[6] Trivedi, S., Kumar, S., Sharma, S.C., *et al.*: 'Biosensing application of multiwall boron nitride nanotube-based nanoresonator for detecting various viruses', *IET Nanobiotechnol.*, 2015, **9**, (5), pp. 259–263
[7] Chen, X., Pan, Y., Liu, H., *et al.*: 'Label-free detection of liver cancer cells by aptamer-based microcantilever biosensor', *Biosens. Bioelectron.*, 2016, **79**, pp. 353–358
[8] Etayash, H., Khan, M.F., Kaur, K., *et al.*: 'Microfluidic cantilever detects bacteria and measures their susceptibility to antibiotics in small confined volumes', *Nat. Commun.*, 2016, **7**, p. 12947
[9] Mathew, R., Ravi Sankar, A.: 'A review on surface stress-based miniaturized piezoresistive Su-8 polymeric cantilever sensors', *Nano-Micro Lett.*, 2018, **10**, (2), p. 35
[10] Lang, P.H., Loizeau, F., Hioufeige, A., *et al.*: 'Piezoresistive membrane surface stress sensors for characterisation of breath samples of head and neck cancer patients', *Sensors*, 2016, **16**, (7), p. 1149
[11] Firdaus, S.M., Azid, I.A., Sidek, O., *et al.*: 'Enhancing the sensitivity of a mass-based piezoresistive micro-electro-mechanical systems cantilever sensor', *Micro-Nano Lett., Inst. Eng. Technol.*, 2010, **5**, pp. 85–90
[12] Yoshikawa, G., Akiyama, T., Gautsch, S., *et al.*: 'Nanomechanical membrane-type surface stress sensor', *Nano Lett.*, 2011, **11**, (3), pp. 1044–1048
[13] Satyanarayana, S., McCormick, D.T., Majumdar, A.: 'Parylene micro membrane capacitive sensor array for chemical and biological sensing', *Sens. Actuators. B-Chem.*, 2006, **115**, (1), pp. 494–502
[14] Tsouti, V., Filippidou, M.K., Boutopoulos, C., *et al.*: 'Self-aligned process for the development of surface stress capacitive biosensor arrays', *Sens. Actuators. B-Chem.*, 2012, **166–167**, pp. 815–818
[15] Loizeau, F., Akiyama, T., Gautsch, S., *et al.*: 'Comparing membrane- and cantilever-based surface stress sensors for reproducibility', *Sens. Actuators. A-Phys.*, 2015, **228**, pp. 9–15
[16] Xiao, W., Huang, C., Xu, F., *et al.*: 'A simple and compact smartphone-based device for the quantitative readout of colloidal gold lateral flow immunoassay strips', *Sens. Actuators. B-Chem.*, 2018, **266**, pp. 63–70
[17] Shahhoseini, E., Ramachandran, P., Patterson, W.R., *et al.*: 'Determination of dose enhancement caused by aunps with Xoft(®) axxent(®) electronic (ebx™) and conventional brachytherapy: in Vitro study', *Int. J. Nanomed.*, 2018, **13**, pp. 5733–5741
[18] Guterman, T., Ing, N.L., Fleischer, S., *et al.*: 'Electrical conductivity, selective adhesion, and biocompatibility in bacteria-inspired peptide–metal self-supporting nanocomposites', *Adv. Mater.*, 2019, **31**, (10), p. 1807285
[19] Shen, M., Duan, N., Wu, S., *et al.*: 'Polydimethylsiloxane gold nanoparticle composite film as structure for aptamer-based detection of vibrio parahaemolyticus by surface-enhanced Raman spectroscopy', *Food Anal. Method*, 2019, **12**, (2), pp. 595–603
[20] Sang, S., Witte, H.: 'A novel pdms micro membrane biosensor based on the analysis of surface stress', *Biosens. Bioelectron.*, 2010, **25**, (11), pp. 2420–2424
[21] Zhao, D., Zhang, Q., Liu, Y., *et al.*: 'Highly sensitive and flexible strain sensor based on aunps/cnts' synergic conductive network', *Appl. Nanosci.*, 2019, **9**, pp. 1–10
[22] El-Naggar, M.E., Shaheen, T.I., Fouda, M.M.G., *et al.*: 'Eco-friendly microwave-assisted green and rapid synthesis of well-stabilized gold and core–shell silver–gold nanoparticles', *Carbohydr. Polym.*, 2016, **136**, pp. 1128–1136
[23] Cha, M., Shin, J., Kim, J.-H., *et al.*: 'Biomolecular detection with a thin membrane transducer', *Lab Chip*, 2008, **8**, (6), pp. 932–937
[24] Jian, A., Tang, X., Feng, Q., *et al.*: 'A pdms surface stress biosensor with optimized micro-membrane: fabrication and application', *Sens. Actuators. B-Chem.*, 2017, **242**, pp. 969–976
[25] Zeinabad, H.A., Ghourchian, H., Falahati, M., *et al.*: 'Ultrasensitive interdigitated capacitance immunosensor using gold nanoparticles', *Nanotechnology*, 2018, **29**, (26), p. 1265102
[26] Sang, S., Witte, H.: 'Fabrication of a surface stress-based PDMS micro-membrane biosensor', *Microsyst. Technol.*, 2010, **16**, (6), pp. 1001–1008
[27] Chen, S., Chu, L., Chen, T.: 'Colorimetric detection of active botulinum neurotoxin using Cu 2 + mediated gold nanoparticles agglomeration', *Sens. Actuators. B-Chem.*, 2016, **235**, pp. 563–567
[28] Zhang, J., Ji, H.: 'An anti *E. coli* o157:H7 antibody-immobilized microcantilever for the detection of *Escherichia coli* (*E. coli*)', *Anal. Sci.*, 2004, **20**, (4), pp. 585–587
[29] Wang, J., Morton, M.J., Elliott, C.T., *et al.*: 'Rapid detection of pathogenic bacteria and screening of phage-derived peptides using microcantilevers', *Anal. Chem.*, 2014, **86**, (3), pp. 1671–1678
[30] Taylor, A.D., Yu, Q.M., Chen, S.F., *et al.*: 'Comparison of *E. coli* o157: h7 preparation methods used for detection with surface plasmon resonance sensor', *Sens. Actuators. B-Chem.*, 2005, **107**, (1), pp. 202–208
[31] Thakur, B., Zhou, G., Chang, J., *et al.*: 'Rapid detection of single *E. coli* bacteria using a graphene-based field-effect transistor device', *Biosens. Bioelectron.*, 2018, **110**, pp. 16–22
[32] Yang, D., Zhou, H., Haisch, C., *et al.*: 'Reproducible *E. coli* detection based on label-free sers and mapping', *Talanta*, 2016, **146**, pp. 457–463